State Mixing and Predissociation in the $\tilde{c} \leftarrow \tilde{a}$ Band System of Singlet Methylene Studied by Optical−Optical Double Resonance†

Zhong Wang, Yangsoo Kim,‡ Gregory E. Hall, and Trevor J. Sears*

Chemistry Department, Brookhaven National Laboratory, Upton, New York 11973-5000

Received: February 4, 2008; Revised Manuscript Received: March 24, 2008

In an attempt to characterize the state interactions near the dissociation energy of singlet methylene, the near ultraviolet band system of singlet methylene has been studied using a laser optical-optical double resonance scheme. Spectra terminating in several, previously unobserved, higher bending levels of the $\tilde{c}^1A_1$ state have been detected. The highest energy band has simple rotational structure with lifetime broadened lines and is observed near 32300 cm^{-1}, which is 500 cm^{-1} above the current best estimate for the singlet bond dissociation energy to $CH(^2\Pi) + H(^2S)$. Two lower energy bands exhibit a proliferation of rotationally-labeled double-resonance lines in the vicinity of the bright $\tilde{c}(0,12,0)$ and $\tilde{c}(0,13,0)$ bending levels, indicating that at least 7 and 9 strongly coupled vibronic states participate in each of these bands, respectively. The additional states may be associated with kinks in the adiabatic $\tilde{c}$ state potential along the asymmetric stretching coordinate associated with interactions among $\tilde{c}^1A'$, $\tilde{a}^1A'$, and $3^1A'$ states, as described by Ostojić (*J. Mol. Spectrosc.* 2002, *212*, 130). There is no evidence for lifetime broadening below the singlet dissociation energy; hence we conclude that coupling of spectroscopically accessible singlet CH_2 levels to the triplet manifold is very small.

Introduction

Since the classic experiments by Herzberg and Johns,[1] spectroscopic studies of singlet methylene have been dominated by work on the near infrared and visible $\tilde{b}^1B_1 \leftarrow \tilde{a}^1A_1$, band system.[2–5] In their original work, Herzberg and Johns[1] also reported fragments of a weaker band system in the near ultraviolet region of the spectrum but were unable to make any definite assignments at the time. However, they tentatively assigned the spectrum to absorption from the $\tilde{a}^1A_1$ to the higher energy $\tilde{c}^1A_1$ state and suggested it was weak due to a combination of a small transition dipole moment and predissociation at its short wavelength end. Interest in this spectrum was revived by a series of computational studies by Bunker and Schaefer and co-workers,[6–8] culminating in a full calculation of the theoretical spectrum.[9] Specific vibrational band assignments were made for the early observations and the failure to observe additional bands in the spectrum above 31000 cm^{-1} was tentatively attributed to predissociation. This speculation was supported in a more recent calculation,[10] but is in contradiction to the best available thermochemical data for methylene, which leads to a somewhat higher singlet methylene bond dissociation energy[11] of 31797 ± 27 cm^{-1}, including zero point energy corrections, for $CH_2(\tilde{a}^1A_1) \rightarrow CH(X^2\Pi) + H(^2S)$. The predissociation might involve crossing to the methylene triplet manifold, accessing the lower energy $C(^3P) + H_2(^1\Sigma)$ asymptote, but the small spin−orbit coupling in CH_2 makes this explanation questionable.

The precise dissociation energy of singlet methylene has been the subject of renewed interest recently as it is crucial to the energetics of the global potential energy surface for the reaction $C(^1D) + H_2 \rightarrow CH + H$. This reaction plays an important role in combustion and astronomical chemistry and is a prototype for a barrierless insertion reaction involving a long-lived complex intermediate. Kalemos et al.[12] reported state-of-the-art calculations on the lowest four states of CH_2 with an emphasis on establishing accurate minima, and Bussery−Honvault et al.[13,14] computed the global potential surface for different symmetry states and all the dissociation asymptotes. They found good agreement with the lowest experimental singlet dissociation limit, $CH_2(\tilde{a}^1A_1) \rightarrow CH(X^2\Pi) + H(^2S)$, calculating a value of 31425 cm^{-1} including zero point corrections, somewhat higher than Ostojić,[10] and a more recent calculation, specifically focused on characterizing the surface intersections by Liu et al.[15] Liu also calculated the $CH_2(\tilde{a}^1A_1) \rightarrow C(^1D) + H_2$ limit to be only 6.3 kcal (2200 cm^{-1}) higher. The triplet asymptote, $C(^3P) + H_2$, lies 10192 cm^{-1} below the corresponding singlet threshold, from the known carbon atomic energy levels. The multiple conical intersections and non-adiabatic interactions in the vicinity of the first singlet dissociation threshold are expected to be important in the reactive processes,[15] and the high resolution spectroscopy of the $\tilde{c}^1A_1$ state provides an experimental view of this complicated region.

In the present work, we report high resolution studies of bands in the $\tilde{c}^1A_1 \leftarrow \tilde{a}^1A_1$ spectrum of CH_2 using optical−optical double resonance (OODR) spectroscopy, which greatly simplifies the rotational structure of the vibronic bands and allows rotational quantum numbers to be assigned in many cases. We find Doppler-limited rotational structure in vibronic bands extending several bending vibrational quanta higher in the $\tilde{c}^1A_1$ state than the bands reported by Herzberg and Johns, and assigned by Bunker et al.,[8–10] indicating that there is effectively no predissociation in these levels. At energies more than approximately 30000 cm^{-1} above the $\tilde{a}^1A_1$state zero point, the double resonance spectra exhibit a higher level density than is expected on the basis of the calculations,[9] which, however, do not explicitly include state mixing in the region of large C−H

† Part of the "Stephen R. Leone Festschrift".

* Corresponding author. E-mail: sears@bnl.gov. fax: 631-344 5815. Phone: 631-344 4374.

‡ Present address: Department of Physics, Virginia Polytechnic Institute and State University, Blacksburg, VA 24061.

10.1021/jp801038e CCC: $40.75
Published on Web 06/18/2008

bond separation.[10] The onset of line broadening for the double-resonance lines occurs at energies of more than 32 000 cm^{-1} above the zero point level of the $\tilde{a}^1A_1$ state, i.e., above both the most recent thermochemical and theoretical singlet methylene bond dissociation energies. The observed line widths in this energy region correspond to predissociation lifetimes of 1.5−2 ps.

Experiment

The experimental setup is similar to that reported previously.[16] CH_2 radicals were formed by 308 nm, 50 mJ/pulse, excimer laser photolysis of a dilute mixture of ketene in an inert gas (helium or argon) in a glass absorption cell 1.5 m in length and approximately 2.5 cm in diameter. The excimer laser beam size (and total energy) was reduced by aperturing to a circular cross section of approximately 1 cm diameter. Ketene was prepared as needed by dehydration of acetic anhydride over a hot filament in a slow flow system which included a dry ice trap to remove water and unreacted acetic anhydride before the absorption cell. The gas mixture was introduced at a total pressure of 0.9 Torr along the length of the absorption cell and was pumped slowly out through a throttling valve on a central port into a liquid nitrogen trapped mechanical pump. The scanning "pump" laser is the UV output from a frequency-doubled pulsed dye laser (Lumonics HD-300) pumped by the second harmonic output of a Nd:YAG laser (Spectra-Physics GCR-170). The near-infrared "probe" laser is a frequency-modulated cw Ti:sapphire laser (Coherent 899-29), monitoring selected single ã state CH_2 rotational levels via a b̃ ← ã transition in a V-type double resonance scheme. The pump and probe beams were aligned collinearly, with crossed linear polarizations, within the photolysis volume defined by the larger cross-sectional area of the excimer photolysis beam. As the dye laser was scanned, second harmonic UV resonances were detected as transient depletion of the probe signal caused by pumping population out of the probed ã state rotational level to the c̃ state. The pump laser was delayed about 0.4 μs after the photolysis laser pulse, long enough to thermalize the initially hot CH_2 photoproduct rotational distribution prior to the pump pulse. Double resonance signals were encoded in the transient radio frequency signal at the modulation frequency of the probe laser, and detected with a silicon photodiode-based receiver. The demodulated transient signal was averaged with a storage oscilloscope (LeCroy Waverunner) and the digitized oscilloscope output was transferred to a PC for data storage and subsequent analysis. The dye laser fundamental wavelength was also recorded continuously during the scan using a commercial wavemeter (Coherent Wavemaster).

Results

A. Time-Dependent OODR Signals. The observed time-dependent absorption signals with the probe laser fixed at 12206.55 cm^{-1} corresponding to the $\tilde{b}(0,3,0)2_{02} \leftarrow \tilde{a}(0,0,0)2_{12}$ transition for different pump laser wavenumbers are shown in Figure 1a−c. [The vibrational quantum numbers are labeled (ν_1, ν_2, ν_3), with the bending quantum number ν_2 defined in the bent molecule limit for the b̃ state, ($2\nu_2$(bent) = ν_2(linear) − Λ − K_a, with Λ = 2 for the b̃ state), but in the linear molecule limit for the c̃ state to permit comparison with the calculated c̃ ← ã spectrum vibronic structure.[9] The rotational state is labeled by $J_{K_aK_c}$.] In these traces, the photolysis laser creates CH_2 at $t = 0$ μs and the pump laser pulse, resonant with a c̃ ← ã transition involving the same ã state rotational level, occurs at about t = 0.4 μs. The detection phase is such that increased CH_2 absorption corresponds to a negative excursion on the vertical axis in these figures. Panel a shows a prompt depletion of absorption signal induced by the pump laser on a c̃ ← ã resonance near 27750 cm^{-1}. Recovery occurs within ∼100 ns, the time scale for rotational relaxation in the ã state at these pressures, refilling the depleted rotational level from its undepleted neighboring rotational states, and restoring the probe transient waveform toward the non-resonant, or unpumped condition, shown as a dotted line. At shorter pump wavelengths, a larger and non-resonant pump-induced transient of the opposite sign is observed, as can be seen in panels b and c. The increment to the probe absorption signal is due to additional ketene photolysis by the pump laser, producing new CH_2 radicals in a dissociation continuum with an efficiency that changes only slowly with pump wavelength. At pump energy near 30063 cm^{-1}, as illustrated in panel (b), only dissociation of internally excited ketene can account for the production of additional CH_2 radicals, because the singlet dissociation threshold of cold ketene is accurately known to be 30116.2 ± 0.4 cm^{-1} from photofragment excitation spectroscopy.[17–19] In panel c, the pump wavenumber, near 32206 cm^{-1}, is well above the singlet dissociation threshold, and the different shape of the formation and relaxation kinetics reflects a hotter initial rotational state distribution, more similar to that produced by the 308 nm photolysis laser. Against this slowly varying, nonresonant background, sharp depletion signals are still detected, as shown by the differences between solid and dotted lines in Figure 1b,c.

A time-dependent OODR signal is obtained by subtracting the probe signal observed with pump-off from the pump-on signal in the simple case when there is no incremental CH_2 photoproduct produced by the pump laser, as in Figure 1a. When additional CH_2 is produced by the pump laser, the reference case is taken as off-resonant pump, rather than pump blocked. These OODR difference signals are shown in Figure 1d, which can be seen to have the same shape for all three cases: prompt depletion followed by recovery on the collisional time scale. For the plotting of OODR spectra that follow, transient waveforms like these difference signals were constructed at each step of the pump laser scan, and the average in a gate near the time of the pump laser is plotted as a function of the pump wavelength.

B. Double-Resonance Spectra of Vibronic Levels in the $\tilde{c}^1A_1$ State. The frequency of the probe laser was chosen to match a known rovibronic transition in the b̃ ← ã band system[20] and the pump laser was scanned in frequency to excite transitions from the same ã state rotational level to rovibrational levels in the $\tilde{c}^1A_1$ state. On the basis of previous experimental work,[16,21] we initially searched for new spectra with pump laser wavelengths near the predicted positions of successive members of the bending vibrational progression[9] of the c̃−ã system. Examples of the OODR spectra terminating in the $\tilde{c}^1A_1$ (0,10,0), $\tilde{c}^1A_1$ (0,12,0) and $\tilde{c}^1A_1$ (0,14,0) levels are shown in Figures 2–5.

(i) $\tilde{c}^1A_1$(0,10,0) and $\tilde{c}^1A_1$(0,11,0). Figure 2 shows a spectrum obtained when scanning the pump laser through the wavelength region corresponding to $\tilde{c}^1A_1$(0,10,0) while the probe laser was fixed on the $2_{02}-2_{12}$ line of the $\tilde{b}(0,3,0) \leftarrow \tilde{a}(0,0,0)$ transition at 12206.55 cm^{-1}. Transitions in Figure 2 therefore all originate in ã(0,0,0) 2_{12} and the wavenumber scale in this and the other figures has been converted to upper state energy using the known ã(0,0,0) energy levels.[22] According to the expected b-type selection rules,[23] allowed transitions in the c̃ ← ã system from 2_{12} can go to the rotational levels 1_{01}, 2_{21}, 3_{03} and 3_{21} in the upper vibronic level, neglecting any ΔK_a changes larger than 1, on the assumption that they will be weaker. Figure 2 shows

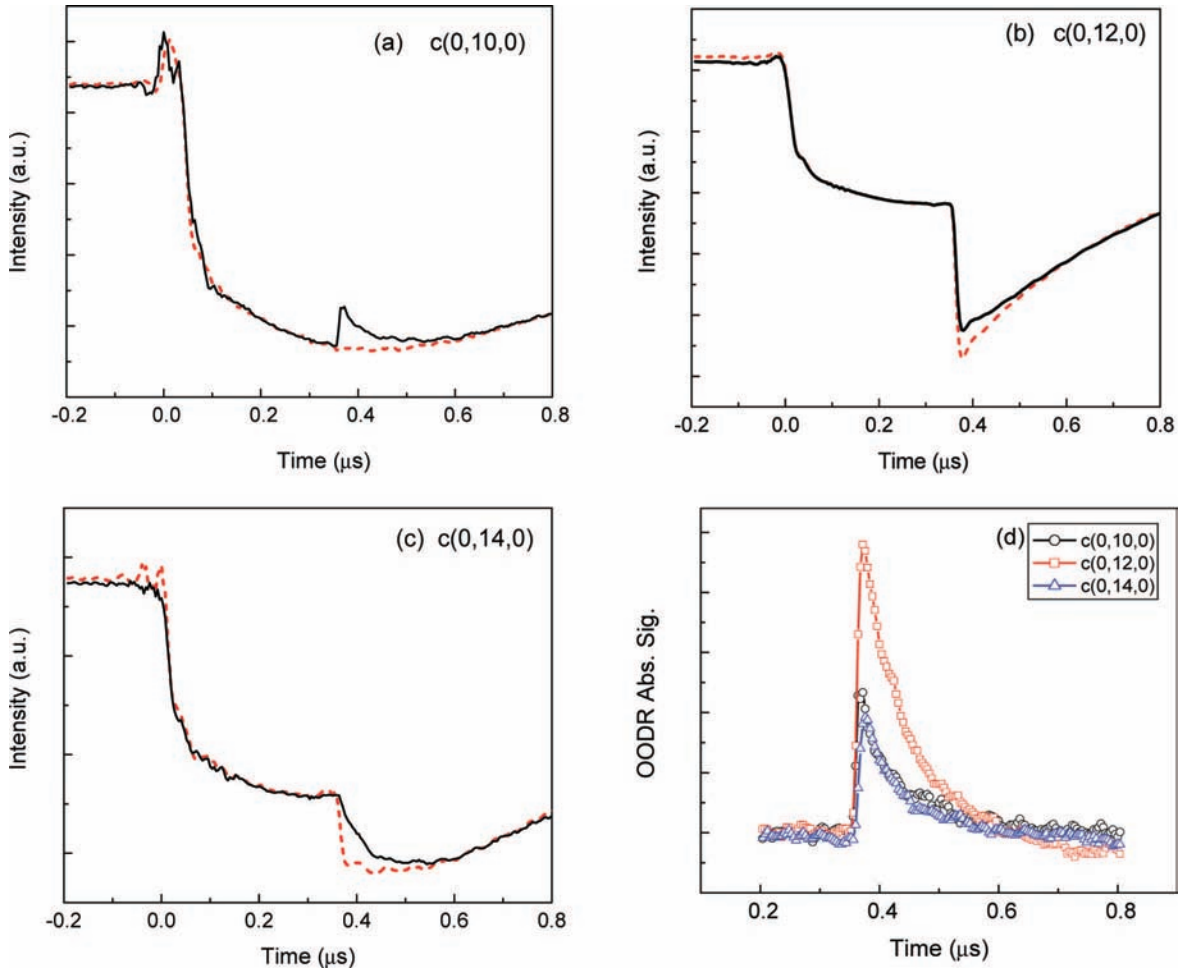

Figure 1. Time-dependent OODR signals with the probe laser fixed at 12206.55 cm^{-1} corresponding to the $\tilde{b}(0,3,0)2_{02} \leftarrow \tilde{a}(0,0,0)2_{12}$ transition. The solid lines show the signals when the pump laser is at (a) 27750.2 cm^{-1}, (0,10,0), (b) 30062.76 cm^{-1}, (0,12,0), and (c) 32205.68 cm^{-1}, (0,14,0) respectively. Dashed lines are background signals for the pump laser blocked (a) or off-resonance (b) and (c). (d) shows the OODR signals which were obtained by subtracting the background (dashed line) signal from the resonant (solid line) signals shown in panels a−c.

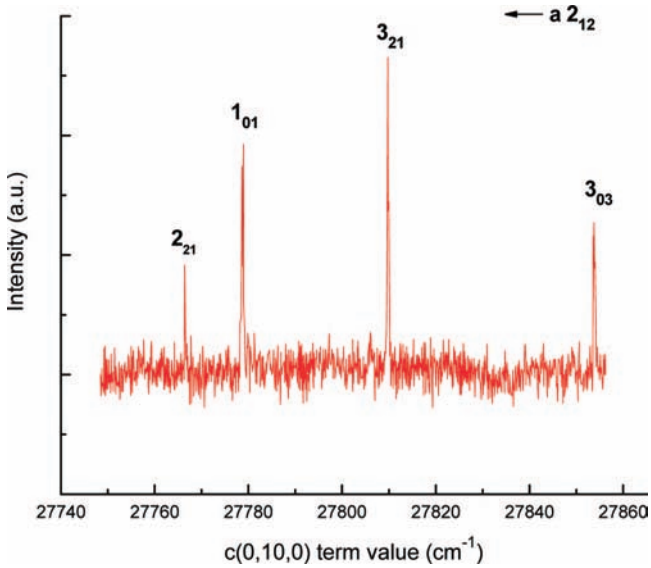

Figure 2. Optical double resonance spectra to levels in $\tilde{c}(0,10,0)$. The horizontal axis is the upper state energy calculated by adding the UV laser wavenumber to the known energy[22] of the probed level ($\tilde{a}(0,0,0)2_{12}$). Only the expected $\Delta J = 0, \pm 1$, $\Delta K_a = \pm 1$ transitions are observed.

four absorption lines were indeed detected and their assignments are given in Table 1. In previous work, transitions to several

TABLE 1: Energies Observed by OODR in the $\tilde{c}(0,10,0)$ Region

$\tilde{c}$ state	$\tilde{c}$ term value (cm^{-1})	$\tilde{c}-\tilde{a}(2_{12})^a$	$\tilde{\nu}$ (cm^{-1})^b	ΔE (cm^{-1})^c
3_{03}	27853.80	27794.24		
3_{21}	27809.76	27750.20	27750.3	−0.1
1_{01}	27778.92	27719.36	27719.2	0.2
2_{21}	27766.44	27706.88	27707.1	−0.2

[a] Spectroscopic transition energy[22] from $\tilde{a}(0,0,0)2_{12}$ at 59.56 cm^{-1}. [b] Wavenumber reported by Herzberg and Johns.[1] [c] Difference between current measurement and ref 1.

$K_a = 0$ rotational levels in the $\tilde{c}^1A_1(0,10,0)$ vibronic level were found using a different optical-optical double resonance scheme.[21] Comparing the results, the absolute energies of the two replicated excited state level measurements were found to be approximately 0.35 cm^{-1} higher in the present work. We now suspect an error in the absolute calibration of the internal wavemeter in the Coherent 899-29 laser to be responsible for this difference. In the ladder-type double resonance scheme used in the previous work, both laser frequencies entered into the $\tilde{c}$ state energy measurement. Checks of the wavemeter used to measure the wavelength of the pulsed dye laser fundamental in the current (and previous) work showed agreement with previously published measurements. Of the newly observed $K_a = 2$ levels, both match lines reported by Herzberg and Johns[1] as shown in Table 1. The $\tilde{c}\ 3_{03}-\tilde{a}\ 2_{12}$ absorption line was not

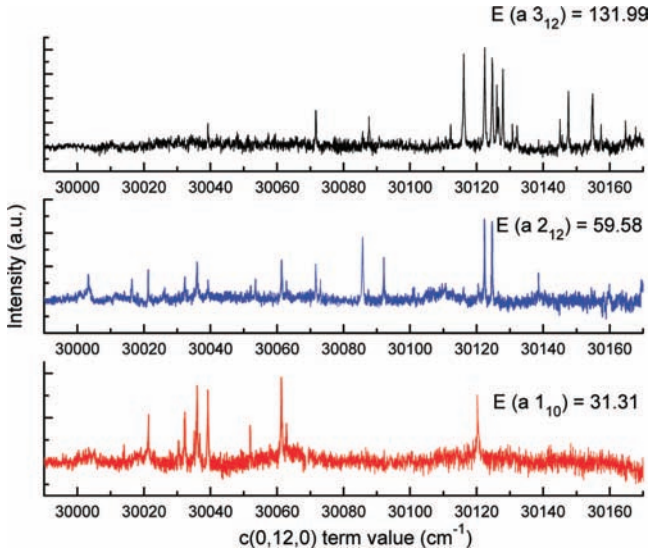

Figure 3. Optical double resonance spectra involving the c̃(0,12,0) level, showing the greater complexity seen at energies closer to the dissociation limit, even for the lowest rotational levels.

reported by Herzberg and Johns, probably due to limitations of sensitivity in their measurements.

The c̃ $^1A_1(0,11,0)$ level was characterized previously.[16] Double resonance spectra terminating in this level also showed simple structure, containing few additional features beyond the expected number of lines. We confirmed this by scanning a section of the spectrum using the present technique, which is better suited to extended spectroscopic searches.

(ii) c̃ $^1A_1(0,12,0)$. Continuing to the higher energy region of the c̃ $^1A_1(0,12,0)$ state, Figure 3 shows double resonance spectra originating in the rotational levels ã(0,0,0) 1_{10}, 2_{12} and 3_{12}. We list the observed lines in Table 2. One immediately notices that there are about 8 times more lines above our background noise level than expected from the rotational levels of a single vibronic state. From the 1_{10} initial level, not 2, but 16 double resonance lines are observed, half of which should terminate in upper 1_{01} rotational levels and the other half in 2_{21} levels. Double resonance spectra from the 2_{12} initial level may have transitions to these same c̃ state levels plus 3_{03} and 3_{21}. Indeed, we observe 33 lines in the 2_{12} spectrum, corresponding to all 16 levels seen in the 1_{01} spectrum and 17 more, approximately the number of expected 3_{03} and 3_{21} levels in 8 coupled vibronic levels. Of the 28 lines identified in the weaker 3_{12} probe spectrum, only two definitely match observed c̃ state 2_{21} levels (six must be too weak to see), only 7 of the expected 16 transitions to 3_{03} and 3_{21} levels are detected, and 16 new transitions are observed. Half of these new transitions likely terminate in 4_{23} levels. The others may be $\Delta K = 3$ transitions to 4_{41} levels with enhanced visibility through stronger Coriolis interactions at higher total angular momentum, or less likely, due to additional 4_{23} levels derived from a larger number of significantly mixed vibronic levels as the total angular momentum increases. A comparison of ortho-(3_{12}) and para-(3_{13}) CH_2 levels in the c̃(0,12,0) state region is shown in Figure 4, using probe transitions out of 3_{12} and 3_{13} rotational levels in the ã state. The energy levels are obviously different in detail but share a similar line density.

We note that all the observed lines associated with the c̃(0,12,0) state have line widths (FWHM) of approximately 0.3−0.4 cm^{-1} as expected on the basis of the combined Doppler and pump laser widths. There is thus no evidence for lifetime broadening with lifetimes shorter than approximately 50−100 ps, at which point additional broadening should have been observed.

Comparing the present observations to Herzberg and Johns[11] spectrum, we find good agreement with their measurements between 29976 and 30005 cm^{-1}, but we did not find any features that correspond to those listed in their work below 29976.46 cm^{-1} and they did not report any features above 30035.37 cm^{-1} where we observed many. We assume that lines listed in the earlier work below 29976.46 and above the (0,11,0) region[16]

TABLE 2: Observed Double Resonance Transitions Terminating in the c̃(0,12,0) Region[a]

1_{01}, 2_{21} ← 1_{10}	1_{01}, 2_{21}, 3_{03}, 3_{21} ← 2_{12}	2_{21}, 3_{03}, 3_{21}, 4_{23} ← 3_{12}	2_{02}, 2_{20}, 3_{22}, 4_{04}, 4_{22} ← 3_{13}[b]
		30167.79	
		30164.75	
	30159.88		
		30157.39	30157.28
		30154.87	30150.84
		30147.57	30144.82
		30145.71	
		30145.07	
		30141.87	
	30138.56	30138.67	30136.06
		30130.73	30131.42
		30127.87	30129.72
		30126.53	
		30126.05	
	30124.64	30124.67	
	30122.34	30122.49	
30120.23	30120.42		30114.54
	30116.1	30116.13	30106.42
		30112.17	30105.28
	30101.20		30104.50
	30092.08		30103.68
		30090.67	30099.28
	30087.42	30087.69	30090.34
	30085.74	30085.79	30087.30
	30073.04		30085.98
	30071.62	30071.61	30082.68
30067.49	30067.49		30078.06
30063.83	30063.83		30076.78
30062.79	30062.79		30072.38
30061.35	30061.35		30069.24
	30053.54		30067.72
30051.95	30052.14		30066.86
		30048.03	30053.50
30039.19	30039.28	30039.29	30038.46
30036.73	30036.50		
30035.93	30035.90		
30035.11	30035.10		
30032.31	30032.32		
30030.37	30030.46	30030.29	
	30026.24		
30021.33	30021.26		
	30018.16		
	30016.46		
30014.03	30014.12		
30003.39	30003.30		
	30000.84		
	29997.16		
29995.79	29995.70		

[a] Converted to upper state term energies in cm^{-1} using the known ã(0,0,0)$^1A_1$ state term energies for 1_{10}, 2_{12} and 3_{12}.[22] Probe transitions are $0_{00}-1_{10}$ at 12188.33, $2_{02}-2_{12}$ at 12206.58 and $3_{03}-3_{13}$ at 12205.06 cm^{-1} in the b̃(0,3,0)−ã(0,0,0) band.[4] [b] Levels observed in the 3_{13} (para-CH_2) spectrum are approximately aligned to match those of the ortho-CH_2 spectrum, but rotational assignments are not possible because only one rotational level was probed.

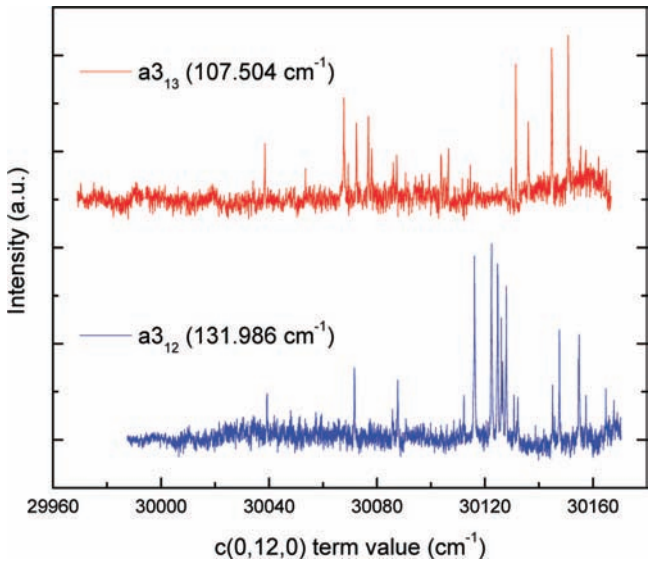

Figure 4. Double resonance spectra comparing ortho-(via 3_{12}) and para-(via 3_{13}) levels in the c̃(0,12,0) region. The energy levels are different, but the overall number of coupled levels is similar.

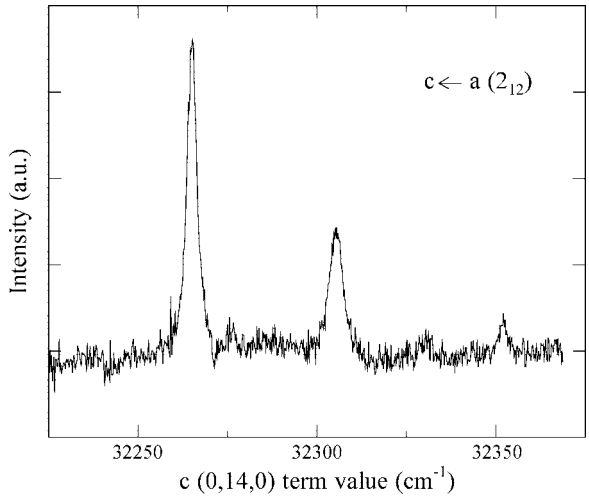

Figure 5. Predissociation broadened transitions in the c̃(0,14,0) region near 32200 cm^{-1}. The three observed transitions originate in the ã(0,0,0) $_1A_12_{12}$level with an energy 59.56 cm^{-1} above the zero point level of the state. The measured energies are 32265.08, 32 05.10 and 32352.56 cm^{-1}. The stronger two lines have measured widths (FWHM) of 2.7 and 3.2 cm^{-1}.

must be due to absorption from $K_a = 2$ or higher levels not investigated in the current work.

(iii) c̃ $^1A_1$(0,13,0). The observations are remarkably similar at the energy of the next bending level, c̃ $^1A_1$(0,13,0). We do not show examples of the spectra, but Table 3 summarizes the measured line positions. Herzberg and Johns[1] reported no absorption lines in this region and for this reason it was previously speculated that singlet CH_2 dissociated somewhere just above the (0,12,0) energy level. However, we find the double resonance spectra have similar strength and vibronic complexity to that observed for the c̃(0,12,0) level, and we continue to find no indication of broadening beyond the expected convolution of Doppler and laser line widths in the c̃(0,13,0) region spectra. Weaker probe transitions were used for these measurements, and precise comparisons of line densities are dependent on our consequent ability to discern weak depletion signals against the background noise level. We note, however, that 9 pairs of closely coincident transitions are identified in

TABLE 3: Observed Double Resonance Transitions Terminating in the c̃(0,13,0) Region[a]

1_{11}, 2_{11} ← 1_{01}	2_{11}, 3_{13}, 4_{13} ← 3_{03}
	31271.97
	31268.19
	31265.77
	31263.19
	31263.19
	31260.33
	31258.69
	31252.29
	31250.23
	31246.45
	31239.53
	31237.31
31231.43	
	31228.31
31222.07	31221.93
	31214.01
	31209.61
	31206.67
31206.19	
	31201.01
31187.17	31187.13
31184.13	31184.13
31177.47	31177.53
31170.39	
31168.51	31168.47
31163.65	31163.59
	31160.63
31157.57	31157.65
31150.61	31150.77
31142.65	
	31138.07
31115.81	31115.83
31113.49	
31097.41	

[a] Converted to upper state term energies in cm^{-1} using the known ã(0,0,0) $^1A_1$ state term energies for 1_{01}, 3_{03}.[22] Probe transitions are $1_{11}-1_{10}$ at 11693.459 and $3_{13}-3_{03}$ at 11703.863 cm^{-1} in the ã(0,10,0)−ã (0,0,0) band.[5]

the double resonance spectra originating from 1_{01} and 3_{03} levels, requiring at least 9 strongly mixed vibronic levels, each with a 2_{12} rotational state in the vicinity of the (0,12,0) bright state. The observation of similar line densities in two levels approximately 1000 cm^{-1} apart near to the dissociation limit is noteworthy. The sum of the coupling of the bright bending levels of the c̃ state to bend-stretch combination levels and nonadiabatic coupling to levels of the other electronic states in the region[10,15] is apparently strong in this energy region but not elsewhere. Extensive scans at wavelengths corresponding to energies between these two bending vibrational levels for spectra originating in the ã $^1A_14_{14}$ level resulted in no additional observed double resonance lines, indicating the intensity in this band system is carried in the bending vibrational progression, as predicted by Yurchenko et al.[9]

(iv) c̃ $^1A_1$(0,14,0). Moving higher still in energy in the c̃ state manifold, Figure 5 shows double resonance spectra in the region of the c̃ $^1A_1$(0,14,0) level obtained via the 2_{12} probe level. The multiple lines attributed to mixing with multiple vibronic levels at lower energy are now gone, and the few rotational transitions that are observed are clearly broadened by predissociation. The observed features at 32265.08, 32305.10 and 32352.56 cm^{-1} are above the thermochemically estimated singlet bond dissociation energy of approximately 31800 cm^{-1}, and the observed broadening is consistent with a singlet dissociation limit clearly below 32265 cm^{-1} From the measured broadening, we estimate

a lifetime of between 1.5 and 2.0 ps for these levels. The second line in Figure 5 is measurably broader than the first, 3.2 compared with 2.7 cm^{-1} (full width half-maximum) with an estimated error of less than 0.2 cm^{-1}, indicating a shorter lifetime, and the third (highest energy) line is too weak for its width to be measured reliably. Although it is tempting to explain the observed increase in width with energy by the approach to the top of a barrier, the transitions almost certainly terminate in different J and/or K_a levels making direct comparisons difficult. Extensive OODR scans probing $\tilde{a}(0,0,0)3_{03}$ were made at wavelengths corresponding to upper state energies between 31275 and 31960 cm^{-1} and probing $\tilde{a}(0,0,0)2_{02}$ between the (0,13,0) and (0,14,0) levels, but only the three broad lines shown in Figure 5 have so far been found. We are anxious to resume our study of the (0,14,0) band using other probe transitions, and to look for the (0,15,0) band in the future, when our frequency doubler is repaired.

Comparing the broadened rotational structure with that shown in Figure 2 for $\tilde{c}(0,10,0)$, we may tentatively assign the first and third lines in the (0,14,0) spectrum to 1_{01} and 3_{03} with a spacing of 87.5 cm^{-1} compared to 74.9 cm^{-1} in (0,10,0). This would require either shorter bond lengths or, more likely, a bent structure. At higher energies, a Franck−Condon picture results in smaller bond angle (more bent) configuration in a bent to linear transition. Future measurements on other probe levels or using, for example, laser polarization dependent measurements[24] should permit rotational level assignments to be made.

Discussion

It now seems clear that the reason Herzberg and Johns[1] did not observe UV transitions to the c̃ $^1A_1(0,12,0)$ and (0,13.0) states is not predissociation, but rather fragmentation of these bright states into multiple weaker, but sharp lines. Both of these bright states are strongly mixed with a comparable number of background states (at least 7), even though no comparable mixing is observed in lower or even higher bending states. We note that even the simplest OODR spectra of these bands, i.e., those derived from 1_{10} and 1_{01}, respectively, do not display a simple pattern of lines that lend themselves to rotational assignments within distinct vibronic states. In a simple picture, the (0,12,0) and (0,13,0) energy levels seen might be considered to be derived from diagonalization of at least an 8×8 matrix for each upper state J. Because the rotational spacings are different for each zero-order vibronic level and the couplings may contain J-dependent matrix elements the simple regular pattern of pairs of rotational levels is lost. Additional experimental information will be accessible in future experiments from measurement of the polarization dependence of the OODR spectra. This should provide information on ΔJ for transitions we have been unable to confirm with double resonance scans using different probe transitions.[24] We plan to do this in the future. Even with secure J assignments for each observed rovibronic energy level in this region, we do not anticipate that a clear pairing of vibronic and rotational assignments will be evident because the vibronic character of the spectroscopically accessible states will vary with the rotational quantum number.

The origin of the increased state mixing in the (0,12,0) and (0,13,0) is clearly of interest. A possible explanation comes from the calculations of Ostojic.[10] Close to the energies of these bending states, the asymmetric stretching potential, corresponding to the approach to the lowest singlet CH + H dissociation asymptote suffers multiple avoided crossings with the ã and 3s Rydberg states. The resulting adiabatic surfaces exhibit unusual kinks and flattening that would be expected to lead to a large increase in density of stretching levels in the region. At still higher energies, the potentials revert to a more normal smooth approach to dissociation. Ostojic did not report any calculations of the vibrational structure associated with these surfaces. Other calculations of vibronic structure in the c̃ state, as computed[9] from the c̃ state potential of Bunker et al.[8] for example, do not take into account the unusual shape of the stretching potential at these energies. Their potential was not evaluated at CH distances large enough to sample the crossings with the dissociative $3^1A'$ or the ã state, between 1.6 and 2.0 Å.[10,15] Instead, a smooth functional form out to the dissociation limit was assumed. We speculate that a denser set of vibronic levels near these surface crossings may account for the localized mixing observed in the double resonance spectra and we plan to calculate the vibronic levels including the effects of multiple surfaces in this region in the future.

The absence of any discernable predissociation broadening below the singlet dissociation threshold argues that there is negligible coupling to the triplet manifold; i.e., spectroscopically accessible singlet character levels in CH_2 are not measurably coupled to the triplet continuum corresponding to the dissociation to $C(^3P) + H_2$ that lies well below this energy. The observation of lifetime broadened levels at energies only 500 cm^{-1} above the estimated dissociation limit implies tunneling through a barrier in the exit channel to dissociation Future measurement of velocity-resolved H atom products produced near the dissociation threshold could permit a precise measurement of the dissociation energy.[25−27] Alternatively, rotationally resolved laser-induced fluorescence of the CH radical product could also bracket the dissociation energy within the energies of successive CH rotational levels as has been done for HCO produced in the dissociation of H_2CO.[28]

Conclusions

The near ultraviolet band system of singlet methylene has been studied using a laser optical-optical double resonance scheme. Several new bands beyond the short wavelength limit of Herzberg and Johns' spectrum were observed. At the lower energy region of the present observations, the bands showed considerable fragmentation of the bright bending states (0,12,0) and (0,13,0). The extra complexity is consistent with anharmonic coupling to an increasing density of stretching and bend-stretch combination states in a region where the adiabatic c̃ potential changes slope and electronic character near conical intersections. The increased line density may explain the apparent disappearance of absorption lines before the dissociation limit in Herzberg's spectrum, because the oscillator strength is diluted among many extra rovibronic levels. Finally, broadened lines appear in a vibronic band near 32300 cm^{-1}, which is 500 cm^{-1} above the current best estimate for the singlet bond dissociation energy to $CH(^2\Pi) + H(^2S)$. Because there is no evidence for dissociation broadening below this energy, we conclude that coupling of spectroscopically accessible singlet CH_2 levels to the triplet manifold is very small.

Acknowledgment. We thank Prof. R. W. Field (MIT) and Hua-Gen Yu (Brookhaven) for helpful discussions on various topics related to this work. This work was performed at Brookhaven National Laboratory under Contract No. DE-AC02-98CH10886 with the U.S. Department of Energy and supported by its Division of Chemical Sciences, Office of Basic Energy Sciences.

References and Notes

(1) Herzberg, G.; Johns, J. W. C. *Proc. R. Soc., London, Ser. A* **1966**, *295*, 107.

(2) Kobayashi, K.; Pride, L. D.; Sears, T. J. *J. Phys. Chem. A* **2000**, *104*, 10119.
(3) Kobayashi, K.; Sears, T. J. *Can. J. Phys.* **2001**, *79*, 347.
(4) Hall, G. E.; Komissarov, A. V.; Sears, T. J. *J. Phys. Chem. A* **2004**, *108*, 7922.
(5) Kobayashi, K.; Hall, G. E.; Sears, T. J. *J. Chem. Phys.* **2006**, *124*, 184320.
(6) Yamaguchi, Y.; Schaeffer, H. F., III *J. Chem. Phys* **1997**, *105*, 1819.
(7) Yamaguchi, Y.; Sherrill, C. D.; Schaeffer, H. F., III *J. Phys. Chem.* **1996**, *100*, 7911.
(8) Bunker, P. R.; Jensen, P.; Yamaguchi, Y.; Schaeffer, H. F., III *J. Phys. Chem.* **1996**, *100*, 18088.
(9) Yurchenko, S. N.; Jensen, P.; Li, Y.; Buenker, R. J.; Bunker, P. R. *J. Mol. Spectrosc.* **2001**, *208*, 136.
(10) Ostojic, B. *J. Mol. Spectrosc.* **2002**, *212*, 130.
(11) Ruscic, B.; Pinzon, R. E.; Morton, M. L.; von Laszewski, G.; Bittnet, S. J.; Nijsure, S. G.; Amin, K. A.; Minkoff, M.; Wagner, A. F. *J. Phys. Chem. A* **2004**, *108*, 9979.
(12) Kalemos, A.; Dunning, T. H.; Mavridis, A.; Harrison, J. F. *Can. J. Chem.* **2004**, *82*, 684.
(13) Bussery-Honvault, B.; Honvault, P.; Launay, J.-M. *J. Chem. Phys.* **2001**, *115*, 10701.
(14) Bussery-Honvault, B.; Julien, J.; Honvault, P.; Launay, J.-M. *Phys. Chem. Chem. Phys.* **2005**, *7*, 1476.
(15) Liu, X.; Bian, W.; Zhao, X.; Tao, X. *J. Chem. Phys.* **2006**, *125*, 074306.
(16) Kim, Y.; Komissarov, A. V.; Hall, G. E.; Sears, T. J. *J. Chem. Phys.* **2005**, *123*, 024306.
(17) Chen, I.-C.; Green, J. W. H.; Moore, C. B. *J. Chem. Phys.* **1988**, *89*, 314.
(18) Chen, I.-C.; Moore, C. B. *J. Phys. Chem.* **1990**, *94*, 263.
(19) Chen, I.-C.; Moore, C. B. *J. Phys. Chem.* **1990**, *94*, 269.
(20) Chang, B. C.; Wu, M.; Hall, G. E.; Sears, T. J. *J. Chem. Phys.* **1994**, *101*, 9236.
(21) Kim, Y.; Hall, G. E.; Sears, T. J. *J. Mol. Spectrosc.* **2006**, *240*, 269.
(22) Petek, H.; Nesbitt, D. J.; Darwin, D. C.; Moore, C. B. *J. Chem. Phys.* **1987**, *86*, 1172.
(23) Bunker, P. R.; Jensen, P. *Molecular Symmetry and Spectroscopy*; National Research Council of Canada Press: Ottawa, 1998.
(24) Petrovic, V. S.; Field, R. W. *J. Chem. Phys.* **2008**, *128*, 014301.
(25) Kim, H.; Dooley, K. S.; Johnson, E. R.; North, S. W. *J. Chem. Phys.* **2006**, *124*, 134304.
(26) Hause, M. L.; Yoon, Y. H.; Crim, F. F. *J. Chem. Phys.* **2006**, *125*, 174309.
(27) Hopkins, W. S.; Loock, H.-P.; Cronin, B.; Nix, M. G. D.; Devine, A. L.; Dixon, R. N.; Ashfold, M. N. R. *J. Chem. Phys.* **2007**, 127.
(28) Terentis, A. C.; Kable, S. H. *Chem. Phys. Lett.* **1996**, *258*, 626.

JP801038E